Radiology: Cardiothoracic Imaging

ORIGINAL RESEARCH

Imaging Profile of the COVID-19 Infection: Radiologic Findings and Literature Review

Ming-Yen Ng • Elaine Y. P. Lee • Jin Yang • Fangfang Yang • Xia Li • Hongxia Wang • Macy Mei-sze Lui • Christine Shing-Yen Lo • Barry Leung • Pek-Lan Khong • Christopher Kim-Ming Hui • Kwok-yung Yuen • Michael D. Kuo, MD

From the Department of Diagnostic Radiology (M.Y.N., E.Y.P.L., P.L.K., M.D.K.), Department of Medicine (M.M.S.L., C.K.M.H.), and Medical Artificial Intelligence Lab Program (M.D.K.), University of Hong Kong, Hong Kong; Department of Diagnostic Radiology (M.Y.N.), Department of Clinical Microbiology and Infection Control (J.Y., K.Y.Y.), and Department of Medicine (F.Y., X.L., H.W.), University of Hong Kong-Shenzhen Hospital, Shenzhen, Guangdong, China; Department of Radiology, Queen Mary Hospital, Hong Kong (C.S.Y.L.); and Department of Radiology, Pamela Youde Nethersole Eastern Hospital, Hong Kong (B.L.). Received February 8, 2020; accepted February 12. **Address correspondence to** M.D.K. (e-mail: *mikedkuo@gmail.com*).

Supported by the Shaw Foundation Hong Kong, Michael Seak-Kan Tong, Respiratory Viral Research Foundation Limited, Hui Ming, Hui Hy and Chow Sin Lan Charity Fund Limited, Marina Man-Wai Lee, the Hong Kong Hainan Commercial Association South China Microbiology Research Fund, Sanming Project of Medicine (Shenzhen), and High Level-Hospital Program (Guangdong Health Commission).

Conflicts of interest are listed at the end of this article.

See editorial by Kay and Abbara in this issue.

Radiology: Cardiothoracic Imaging 2020; 2(1):e200034 • https://doi.org/10.1148/ryct.2020200034 • Content code: CH

Purpose: To present the findings of 21 coronavirus disease 2019 (COVID-19) cases from two Chinese centers with CT and chest radiographic findings, as well as follow-up imaging in five cases.

Materials and Methods: This was a retrospective study in Shenzhen and Hong Kong. Patients with COVID-19 infection were included. A systematic review of the published literature on radiologic features of COVID-19 infection was conducted.

Results: The predominant imaging pattern was of ground-glass opacification with occasional consolidation in the peripheries. Pleural effusions and lymphadenopathy were absent in all cases. Patients demonstrated evolution of the ground-glass opacities into consolidation and subsequent resolution of the airspace changes. Ground-glass and consolidative opacities visible on CT are sometimes undetectable on chest radiography, suggesting that CT is a more sensitive imaging modality for investigation. The systematic review identified four other studies confirming the findings of bilateral and peripheral ground glass with or without consolidation as the predominant finding at CT chest examinations.

Conclusion: Pulmonary manifestation of COVID-19 infection is predominantly characterized by ground-glass opacification with occasional consolidation on CT. Radiographic findings in patients presenting in Shenzhen and Hong Kong are in keeping with four previous publications from other sites.

On January 30, 2020, the coronavirus disease 2019 (COVID-19), formerly known as 2019 novel coronavirus (2019-nCoV), was declared to be a global health emergency by the World Health Organization (1). Dramatic measures have been put in place to halt the progression of the virus, and as of February 6, 2020, COVID-19 has infected over 28,000 patients with 564 confirmed deaths (2). Knowledge of COVID-19 is still evolving, but anecdotal evidence is available suggesting that patients can be asymptomatic and infective for up to 14 days (3). It is clear that our understanding of the radiologic features of COVID-19 is incomplete, and as it continues to rapidly spread, there is an urgent need to consolidate the emerging knowledge on its radiologic profile.

In China, the disease center, imaging has been at the forefront of investigation for patients with suspected or confirmed COVID-19 infection. As a result, CT of the chest has been used on an unprecedented scale. Whereas the previous outbreak of severe acute respiratory syndrome (SARS) predominantly induced a spike in chest radiography utilization, the literature on the COVID-19, so far, has mainly focused on the role of CT for identifying patients and assessing disease progression.

Since the initial published cases in Wuhan, COVID-19 has spread widely, including all provinces in China and 19 countries overseas (2).

In this study, we add to the evolving radiologic profile of COVID-19 with the presentation of chest CT and chest radiographic findings of 21 cases in Shenzhen and Hong Kong, China, supplemented with further insight about the timing of symptom onset versus imaging findings, clinical symptoms, and hematologic and biochemical markers, as well as CT and radiographic follow-up imaging. Furthermore, we performed a literature review to provide an up-to-date synthesis of the radiographic portrait of the COVID-19 infection.

Materials and Methods

Study approval was obtained from the institutional review boards of the University of Hong Kong-Shenzhen Hospital, Hong Kong West, and Eastern Cluster. Patients with confirmed COVID-19 infection were identified and

Abbreviations

COVID-19 = coronavirus disease 2019, RT-PCR = reverse-transcription polymerase chain reaction, SARS = severe acute respiratory syndrome

Summary

Chest radiographic and CT findings of 21 patients with confirmed COVID-19 are described along with a literature review of other publications describing the radiologic findings of this novel coronavirus.

Key Points

- Chest radiographic and CT findings of 21 patients with confirmed COVID-19 infection in Shenzhen and Hong Kong are described and compared.
- A literature review and tabulation of the radiographic features in original publications are presented.
- One asymptomatic patient had evidence of consolidation at chest CT.

enrolled in the study. Reverse-transcription polymerase chain reaction (RT-PCR) methods for identifying COVID-19 have been previously described (3). Two additional patients who traveled to Wuhan and with contact history, clinical symptoms, blood results, and negative swabs for other diseases were diagnosed as infected by COVID-19. Written consent was obtained for patients in Shenzhen, while consent requirements were waived for the cases recruited in Hong Kong according to local institutional review board requirements. Eighteen patients were recruited from Shenzhen and three were recruited from Hong Kong. Six patients recruited from Shenzhen have been previously reported, but the radiologic appearances were only briefly mentioned (3). All patients underwent at least one chest CT, while four patients also underwent follow-up CT. Five patients underwent chest radiography, of which three underwent follow-up chest radiography on a daily basis. Two patients underwent six follow-up chest radiographic examinations and one patient underwent 10 follow-up chest radiographic examinations.

Clinical Parameters and Blood Tests

Clinical data, such as symptoms and past medical history, were obtained directly from the patient or through the electronic patient database. Onset of symptoms to time of CT examinations and time interval between CT examinations and chest radiographic examinations were obtained. Hematologic and biochemical blood test results were gathered using the electronic patient record system.

Image Acquisition

Volumetric CT thorax images were acquired at 1-mm slice thickness and reformatted with lung and soft-tissue windows. No intravenous contrast material was administered. Conventional chest radiographs were acquired in the posteroanterior projection at initial presentation. Follow-up films were acquired in the anteroposterior projection. All of the radiologic studies followed usual clinical acquisition parameters according to local protocols.

Image Interpretation

All available CT and radiographic images of the relevant patients were obtained and reviewed by two thoracic radiologists jointly (M.Y.N., 8 years of experience with cardiothoracic fellowship training and E.Y.P.L., 12 years of experience).

CT images were classified as having ground-glass opacities, consolidation, cavitation, or nodular opacities. The distribution of these lung changes was also classified on the basis of *(a)* upper zone predominance, lower zone predominance, or no zonal predominance; *(b)* peripheral or central predominance or neither; *(c)* lobes involved; *(d)* presence of pleural or pericardial effusions; and *(e)* presence of enlarged mediastinal or hilar lymph nodes (defined as a lymph node with a short-axis measurement $\geq$ 10 mm, only on CT). Chest radiographic images were assessed in a similar manner, allowing for technical differences between methods.

Patients with follow-up CT or radiographic images were compared to determine whether there was progression, stability, or improvement of the lung changes.

Radiologic lesions were diagnosed on the basis of the Fleischner Society glossary of terms (4). Ground-glass opacities were defined as an increase in opacification of the lung that does not obscure the blood vessels and airways. Consolidation was defined as a homogeneous opacification that obscures blood vessels and airway walls. A reversed CT halo sign was defined as a rounded area of ground glass surrounded by a complete or almost complete ring of consolidation.

Comparison and Synthesis of Radiographic Findings with Published Literature

Previous publications were searched to obtain a larger consensus of radiographic appearances at chest CT and radiographic examinations. The search terms "Wuhan" and "coronavirus" were used in PubMed for original research publications written in the English language between December 1, 2019, and February 7, 2020. Only publications with $>$ 10 patients were included in the final sample. A total of 56 publications were found. Twenty-eight publications were removed on inspection of the title, and 25 publications were removed based on the review of the abstract and full paper, leaving four eligible publications for detailed review.

Statistical Analysis

Findings are presented as medians and interquartile ranges owing to the small sample size. Categorical variables are described as whole numbers, with percentages in brackets.

Results

Of the 18 patients, 13 were male and eight were female. The patients' ages ranged from 10 to 74 years. All patients were symptomatic, except for one patient who was the child of a family cluster confirmed to have COVID-19. Clinical symptoms, past medical history, history of travel to Wuhan, and hematologic and biochemical results are summarized in Table 1.

Table 1: Patient Characteristics including Travel History, Symptoms, Past Medical History, and Hematologic and Biochemical Findings

Parameter	Value
Sex	
Male	13 (62)
Female	8 (38)
Age (y)	56 (37–65)
Travel to Wuhan	17 (81)
Contact with patient with confirmed COVID-19	3
Symptom	
Fever	19 (90)
Temperature (°C)	38 (37.4–38.4)
Heart rate (beats/min)	90.5 (82.5–103)
Systolic blood pressure (mm Hg)	126 (119.5–150)
Diastolic blood pressure (mm Hg)	78 (74–87.5)
Respiratory rate (breaths per minute)	19 (18–20)
Saturations (%)	97 (96–98)
Cough	10 (48)
Sputum	3 (15)
Hemoptysis	0 (0)
Sore throat	2 (10)
Diarrhea	2 (10)
Chest pain/pleuritic chest pain	1 (5)
Dyspnea	0 (0)
Past medical history	
Diabetes	3 (14)
Hypertension	3 (14)
Chronic obstructive pulmonary disease	0 (0)
Malignancy	0 (0)
Chronic liver disease	1 (5)
Human immunodeficiency virus	0 (0)
Hematologic results	
Hemoglobin (g/dL) (male normal range 13.3–17.1; female normal range 11.5–14.8)	13.8 (13.2–15.3)
White cell count ($\times 10^9$ cells/liter) (normal range 3.9–9.9)	5.3 (4.3–6.2)
Neutrophil count ($\times 10^9$ cells/liter) (normal range 2.0–7.4)	3.33 (3–3.91)
Lymphocyte count ($\times 10^9$ cells/liter) (normal range 1.1–3.6)	1.29 (0.7–1.65)
Platelet count ($\times 10^9$ cells/liter) (normal range 162–341)	169 (148–196)
Prothrombin time (sec) (normal range 11.0–14.5)	12.7 (12.2–13)
Activated partial thromboplastin time (sec) (normal range 26.0–40.0)	36 (34–41)
Biochemistry results	
D-Dimer (mg/mL) (normal range 0.0–0.5)	0.4 (0.26–0.6)
Sodium (mmol/L) (normal range 136–145)	139 (136–141)
Potassium (normal range 3.5–5.1)	3.86 (3.7–4)
Urea (mmol/L) (normal range 2.8–8.1)	4.45 (3.4–5.5)
Creatinine (mmol/L) (normal range 44–80)	72 (55–84)
Albumin (normal range 35.0–52.0)	42.2 (39.4–45.8)
Total bilirubin (normal range 0.0–21.0)	7.0 (5.9–8.8)
Alanine aminotransferase (normal range 0.0–33.0)	22.5 (15.6–34.4)
Aspartate aminotransferase (normal range 0.0–32.0)	25.5 (20.1–35.2)
Lactate dehydrogenase (normal range 135–214)	218 (183–252)
Creatine kinase (normal range 0–170)	78 (69–137)

Note.—Values are given as median and interquartile range for continuous variables and numbers with percentages in parentheses for categorical variables.

Chest CT Findings

Thorax CT examinations were performed at a median of 3 days from onset of symptoms (interquartile range, 1–7 days). Of the 21 cases, two patients had normal chest CT images. The CT lesions and distribution across the 21 reported cases are listed in Table 2. Briefly, the predominant feature was ground-glass opacification (*n* = 18, 86%) followed by consolidation (*n* = 13, 62%) (see Fig 1). In total, 11 cases had predominantly ground-glass opacities, four had mixed appearances, and four had predominantly consolidative changes. The ground-glass and consolidative opacities were peripheral in all patients with lung findings (*n* = 18), apart from one patient who had perihilar ground-glass changes. Eight patients showed lower zone predominance, eight patients showed equal distribution between the upper and lower zones, and three patients showed upper zone predominant changes. Subpleural sparing, pleural effusions, pericardial effusion, cavitation, and mediastinal and hilar lymph node enlargement were not seen in any of the patients.

Ground-glass and consolidative opacities were most frequently seen in the left lower lobe (*n* = 17, 81%), right lower lobe, and left upper lobe (both *n* = 16, 76%), whereas the right middle lobe had the lowest involvement (*n* = 10, 48%) (see Table 2). The reversed CT halo sign was seen infrequently (*n* = 2).

Chest Radiographic Findings

Five patients underwent chest radiographic along with thorax CT examinations (Table

Table 2: CT Chest Findings

Parameter	Value
Symptom onset to first CT scan (days)	3 (1–7)
Lobar involvement	
RUL	14 (67)
RML	10 (48)
RLL	16 (76)
LUL	16 (76)
LLL	17 (81)
CT lung lesion appearances	
Ground-glass opacities	18 (86)
Ground-glass nodules	4 (19)
Consolidation	13 (62)
>50% findings were ground-glass opacities	11
>50% findings were consolidations	4
Equal mix of ground glass and consolidation	4
Cavitation	0
Solid nodules	1*
Pleural effusion	0
Pericardial effusion	0
Enlarged mediastinal or hilar lymph nodes (≥ 10 mm in short axis measurement)	0
No abnormal findings	2
Predominant distribution	
Peripheral	18 (86)
Perihilar	1 (5)
Neither peripheral or perihilar	2†
Upper zone	3 (14)
Lower zone	8 (38)
Similar upper and lower zone involvement	8 (38)

Note.—Values are numbers with percentages in parentheses, unless otherwise specified. LLL = left lower lobe; LUL = left upper lobe; RLL = right lower lobe; RML = right middle lobe; RUL = right upper lobe.
*Appearance consistent with a solitary intrapulmonary lymph node.
† CT showed no abnormalities.

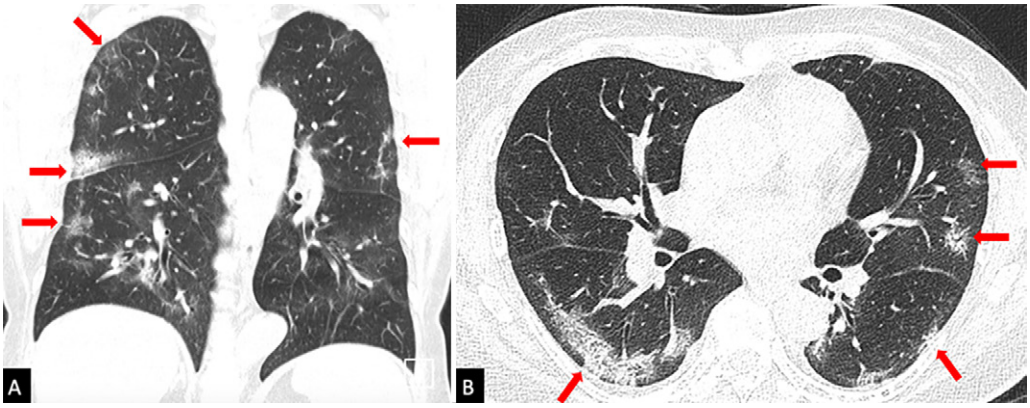

Figure 1: A 65-year-old female patient who had traveled to Wuhan, China, subsequently developing fever and cough 5 days after arrival. She returned to Shenzhen, China, and underwent this chest CT examination 7 days after symptom onset. *A*, Coronal and, *B*, axial CT images show a mixture of ground glass and consolidation in the periphery of the lungs (red arrows), with the absence of pleural effusions, which was the typical appearance of patients with confirmed COVID-19 infection.

3). Of these, two patients showed normal chest radiographic findings, despite also having CT examinations performed on the same day showing ground-glass opacities (Fig 2). The other three chest radiographic examinations showed consolidation. One chest radiographic examination showed lower zone predominance, while the other two chest radiographic examinations did not show any zonal predominance. In these three patients, their chest radiographic examinations did not show the peripheral predominance that was visible on their respective CT examinations.

Table 3: Chest Radiograph Findings in Five Patients

Parameter	Value
Lung changes	
Normal chest radiographic findings	2
Consolidation	3
Predominantly consolidation	2
Bilateral lung involvement	2
Pleural effusion	0
Predominance	
Upper zone	0
Lower zone	1
Similar upper and lower zone involvement	2

CT and Radiographic Follow-up

Four of 21 patients underwent a follow-up CT. Three patients underwent follow-up CT performed 4 days after the initial CT, while one patient underwent follow-up CT 3 days after the initial CT. In one patient, there was a reduction in the consolidation (Fig 3). The second patient had a normal thorax CT examination at presentation. On subsequent CT examinations, the CT findings remained normal with no new lung changes. The third patient's CT showed progression of the lung changes with new ground-glass nodules in other lobes. The preceding ground-glass opacities increased in size, with some peripheral consolidation (Fig 4). The fourth patient showed the previously observed ground-glass opacities becoming smaller areas of consolidation.

Three different patients underwent daily chest radiographic examinations. In two patients, there was progression in the lung consolidation over a period of 3–4 days (Fig 5). Subsequent chest radiographic examinations showed improvement over the following 2 days (Fig 5). The third patient showed no significant changes over an 8-day period.

Literature Review of Radiographic Appearances of COVID-19

We identified four articles (5–8) with more than 10 patients describing the chest radiographic or CT findings of patients

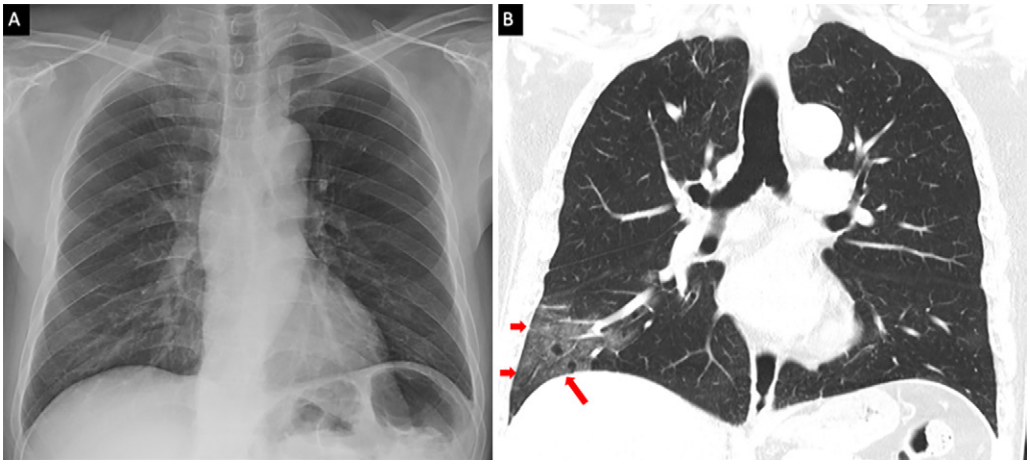

Figure 2: A comparison of, *A*, chest radiograph and, *B*, thorax CT coronal image. The ground-glass opacities in the right lower lobe periphery on the CT (red arrows) are not visible on the chest radiograph, which was taken within 1 hour of the CT.

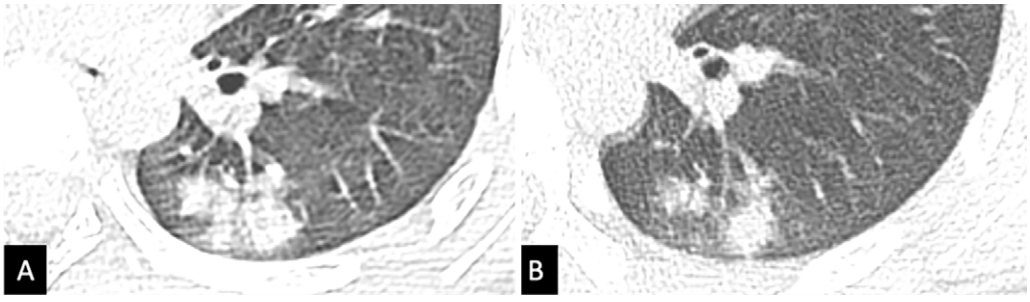

Figure 3: A 10-year-old asymptomatic male child with confirmed COVID-19 infection, who had traveled to Wuhan, China, with his family. *A*, Image shows the initial CT scan at time of presentation, with consolidation in the left lower lobe apical segment. *B*, Image shows mild improvement in the lung consolidation 4 days later.

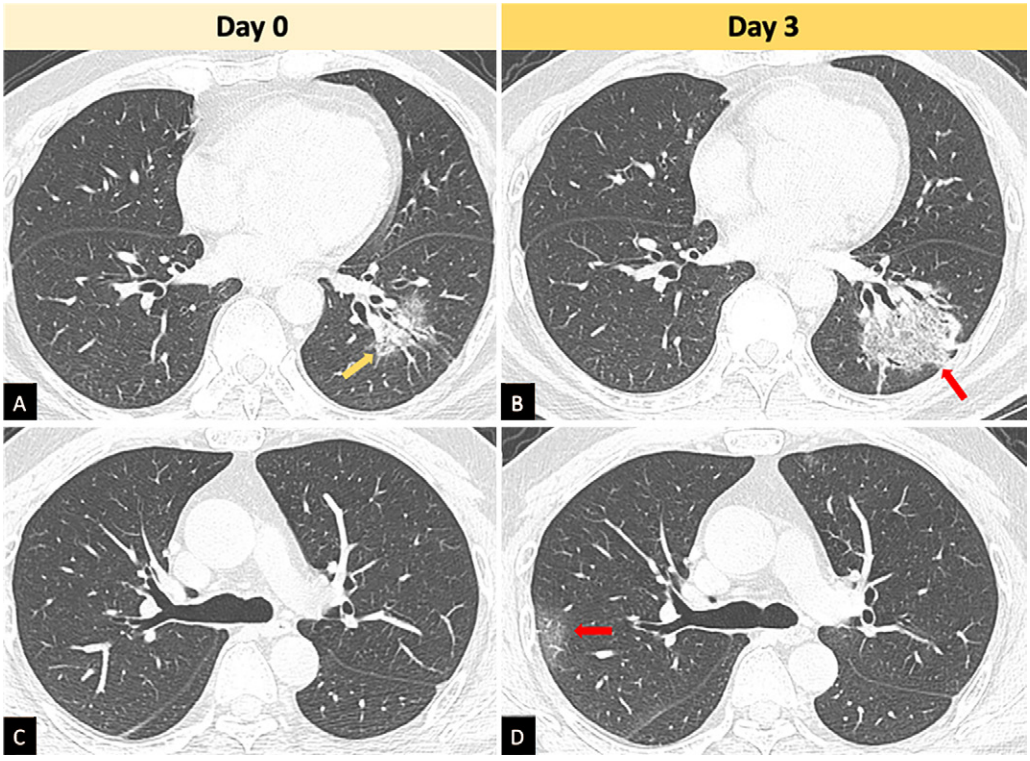

Figure 4: Chest CT follow-up in a patient who had no previous travel to Wuhan, China, but had contact with a patient with confirmed COVID-19 infection. Axial slices from day 0 of presentation to the hospital shows ground-glass opacities in the left lower lobe (arrow, *A*), but not in the right upper lobe (*C*). Subsequently, 3 days later, the follow-up CT showed an increase in the ground-glass changes with some peripheral consolidation (reversed halo, arrow, *B*) and new ground-glass opacities in the right upper lobe periphery (arrow, *D*).

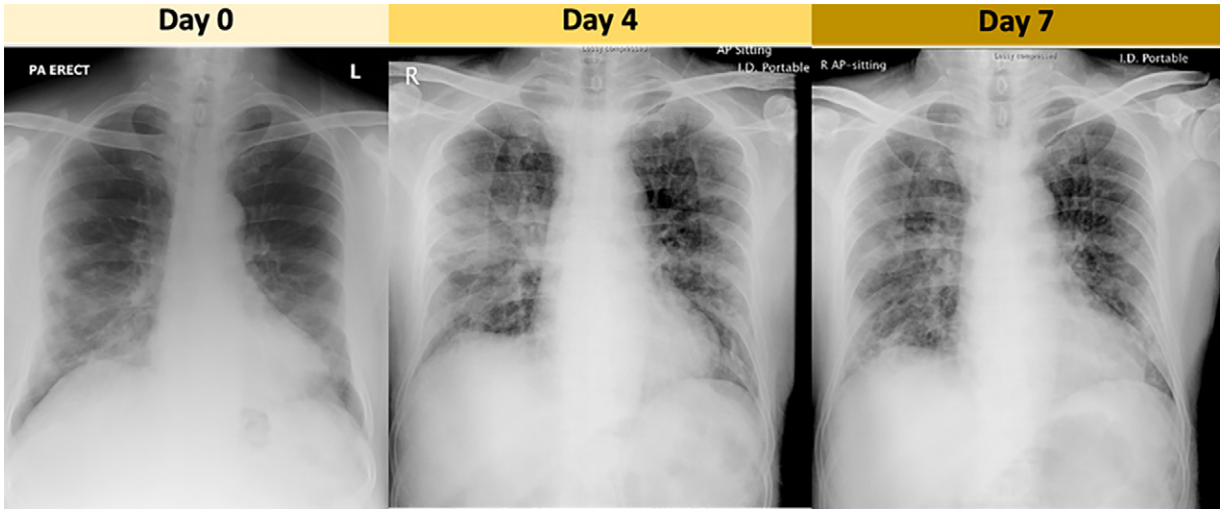

Figure 5: Chest radiographs in an older male patient from Wuhan, China, who traveled to Hong Kong, China. These are three chest radiographs selected out of the daily chest radiographs acquired in this patient. The consolidation in the right lower zone on day 0 persisted into day 4 with new consolidative changes in the right midzone periphery and perihilar region. This midzone change improved on the day 7 radiograph.

infected with COVID-19 (Table 4). The studies had 99 patients, 41 patients, 21 patients, and 51 patients, in chronological order of publication date (from January 30, 2019, to February 6, 2020), with the mean or median age of patients being 50 years. Two studies briefly described the CT appearances of the lung findings, in which they described a predominantly bilateral pneumonia or consolidation. In the study by Huang et al (6) with 41 patients, they described predominantly consolidation in patients in the intensive care unit, while the patients outside the intensive care setting had a mixture of ground-glass opacities and consolidation. In the study by Chen et al (5) with 99 patients, in addition to the CT findings, they found that bilateral pneumonias were the most common finding on chest radiographs. In the article by Chung et al (7), the

Table 4: Comparison of Articles Published before February 7, 2020

Parameter	Current Study	Chen et al (5)	Huang et al (6)	Chung et al (7)	Song et al (8)
No. of patients	21	99	41	21	51
Age (y)	Median 56 (IQR 37–65)	Mean 55.5 (SD 13.1)	Median 49 (IQR 41–58)	Mean 51 (range 29–77)	Mean 49 (range 16–76)
Imaging modality	CT and CXR	CT and CXR	CT only	CT only	CT only
Chest radiographic findings					
Consolidation	60%	100%			
Pleural effusion	0	N/A			
Progression visible	Yes	N/A			
Improvement visible	Yes	N/A			
Normal radiograph	2	0			
CT findings					
Time between onset and first CT (days)	Median 3 (IQR 1–7)	N/A	8	N/A	Classified as (i) ≤ 4 or (ii) > 4
Consolidation (%)	62	100	Typically present	29	59
Ground glass (%)	86	14	Typically present	86	77
Predominant distribution	Peripheral (86%) Lower zone (38%) Similar upper and lower zone (38%)	Bilateral (75%)	Bilateral (98%)	Peripheral (33%) Bilateral (76%)	Peripheral (86%) Bilateral (86%) Lower lobes (90%)
Lymphadenopathy (%)	0	N/A	N/A	0	6
Pleural effusion (%)	0	N/A	N/A	0	6
CT follow-up					
No. of CT follow-up cases	4 patients	1 patient	1 patient	8 patients	13 patients
Time interval between symptom onset and first CT (days)	5–10 (1 patient was asymptomatic)	N/A	8	N/A	Classified as (i) ≤ 4 or (ii) > 4
Time difference between CT examinations (days)	3–4	14	4	1–4 (mean 2.5)	N/A
Improvement, *n* (%)	2 (50)	1 (100)	1 (100)	0 (0)	7 (54)
Progression, *n* (%)	1 (25)	0 (0)	0 (0)	7 (88)	4 (31)
Stable, *n* (%)	1 (25) [Patient had normal CT at presentation]	0 (0)	0 (0)	1 (13) [Patient with normal CT]	2 (15)

Note.—CXR = chest radiography, IQR = interquartile range, N/A = not applicable; SD = standard deviation.

CT findings were typically ground glass (57%) and peripheral distribution (33%). Lung cavitation, discrete pulmonary nodules, pleural effusions, and enlarged lymph nodes were absent. They also found normal chest CT images in 14% of patients. Song et al (8) described predominantly ground-glass opacities (77%) but a larger amount of peripheral distribution (86%) and lower lobe involvement (90%). They further showed that there was improvement in follow-up chest CT examinations in 54% of the patients, contrasting with imaging progression seen in 31% of patients.

Discussion

Our study confirms that ground-glass opacities and consolidation in the lung periphery has been the imaging hallmark in

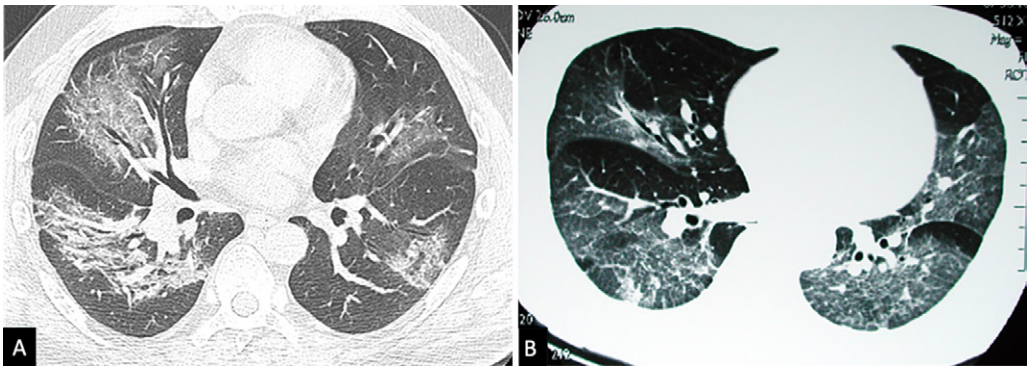

Figure 6: Axial CT images show, *A*, case of COVID-19 and, *B*, a case of severe acute respiratory syndrome from 2003. Both cases demonstrate similar predominantly ground-glass opacities affecting both lungs.

patients with COVID-19 infection. Furthermore, solid pulmonary nodules, cavitation, pleural effusions, and mediastinal and hilar lymph node enlargement were not typically observed. We performed a review of the recent literature to synthesize the findings in 233 patients infected with COVID-19 (including 21 reported herein). All studies have shown consistent findings, with bilateral ground glass and consolidation being the most frequent findings on CT and radiographic examinations. Peripheral predominance of the lung opacities has been also found across studies. Furthermore, we identified one asymptomatic patient with chest CT abnormalities. Despite many potential biases related to patient selection and the retrospective nature of the study, our findings suggest that chest radiography may lack sensitivity to identify some of the manifestations of the COVID-19 infection in the lungs, which are otherwise evident on CT images.

While the disease profile of COVID-19 is dynamic and continues to rapidly evolve, there are still many open questions. As is evident in our synthesis, there are cases where patients with confirmed COVID-19 infection have no chest CT abnormalities, contrasting with subclinical infection presenting with positive imaging findings at CT examinations (7). It is crucial that the clinical impacts of screening asymptomatic patients with chest CT be determined. A more thorough analysis about the existence of any potential benefit on clinical outcomes needs to be addressed against the known financial costs and exposure to ionizing radiation associated with CT scanning.

As more and more suspected cases arise, there are issues with having enough available RT-PCR kits to confirm COVID-19 infection. This has led to chest CT being used to aid diagnosis in the absence of RT-PCR, as demonstrated in a recent case report from China (9). Our experience in the Guangdong province has seen an unprecedented use of CT in an infectious disease outbreak. The power of this tool in helping to raise suspicion as well as to follow the course of the disease is becoming increasingly apparent. In the Guangdong province, chest CT examinations are being requested for every patient suspected of having COVID-19. Thus, in addition to aiding in disease screening and follow-up evaluation, further investigation is also necessary to determine the role of CT in helping guide therapy.

Of note, our cases bear striking similarities to SARS (Fig 6). Both pathogens demonstrate predominantly ground-glass opacities, with consolidation occasionally seen (10,11). The progression of the lung changes of COVID-19 on CT imaging is also similar to SARS, with the ground glass and consolidation getting worse or better over several days (12). This would be expected as the two infectious agents are part of the coronavirus family. SARS had a mortality rate of 9.5% (13), whereas the current novel coronavirus appears to have a mortality rate of around 2%, on the basis of the number of confirmed cases and deaths (2).

Our study had several limitations, but mainly, our sample size is small and our follow-up interval, short. Such limitations preclude the possibility of any deep analysis about potential prognostic imaging variables that could aid in the prediction of worse outcomes. Moreover, it does not address the role of imaging in guiding or monitoring medical therapy in the infected individuals. Nonetheless, our study continues to add knowledge about the disease in a growing number of centers apart from the epicenter of the outbreak in Wuhan. Finally, it also presents chest radiographic findings in a small number of patients, information that was lacking in most of the recent imaging reports of the disease.

In conclusion, we present the CT and chest radiographic findings of 21 patients infected with COVID-19 in Shenzhen and Hong Kong, providing a composite radiologic profile with a systematic review of the current literature.

Acknowledgments: We would like to thank Ambrose Fong and Benedicte Coiffier for their assistance.

Author contributions: Guarantors of integrity of entire study, M.Y.N., J.Y., F.Y., X.L., H.W., M.M.S.L., C.K.M.H., K.Y.Y., M.D.K.; study concepts/study design or data acquisition or data analysis/interpretation, all authors; manuscript drafting or manuscript revision for important intellectual content, all authors; approval of final version of submitted manuscript, all authors; agrees to ensure any questions related to the work are appropriately resolved, all authors; literature research, M.Y.N., E.Y.P.L., B.L., C.K.M.H., M.D.K.; clinical studies, E.Y.P.L., J.Y., F.Y., X.L., H.W., M.M.S.L., B.L., P.L.K., C.K.M.H., K.Y.Y., M.D.K.; experimental studies, E.Y.P.L.; statistical analysis, M.Y.N., M.D.K.; and manuscript editing, M.Y.N., E.Y.P.L., M.M.S.L., C.S.Y.L., P.L.K., M.D.K.

Disclosures of Conflicts of Interest: **M.Y.G.** disclosed no relevant relationships. **E.Y.P.L.** disclosed no relevant relationships. **J.Y.** disclosed no relevant relationships. **F.Y.** disclosed no relevant relationships. **X.I.** disclosed no relevant relationships. **H.W.** disclosed no relevant relationships. **M.M.L.** disclosed no relevant relationships. **C.S.Y.L.** disclosed no relevant relationships. **B.L.** disclosed no relevant relationships. **P.L.K.** disclosed no relevant relationships. **C.K.M.H.** disclosed no relevant relationships. **K.Y.** disclosed no relevant relationships. **M.D.K.** disclosed no relevant relationships.

References

1. World Health Organization. Novel Coronavirus(2019-nCoV) Situation Report - 11. https://www.who.int/docs/default-source/coronaviruse/situation-reports/20200131-sitrep-11-ncov.pdf?sfvrsn=de7c0f7_4. Published January 31, 2020.
2. World Health Organization. Novel Coronavirus(2019-nCoV) Situation Report - 17. https://www.who.int/docs/default-source/coronaviruse/situation-reports/20200206-sitrep-17-ncov.pdf?sfvrsn=17f0dca_2. Published February 6, 2020.
3. Chan JF, Yuan S, Kok KH, et al. A familial cluster of pneumonia associated with the 2019 novel coronavirus indicating person-to-person transmission: a study of a family cluster. Lancet 2020 Jan 24 [Epub ahead of print].
4. Hansell DM, Bankier AA, MacMahon H, McLoud TC, Müller NL, Remy J. Fleischner Society: glossary of terms for thoracic imaging. Radiology 2008;246(3):697–722.
5. Chen N, Zhou M, Dong X, et al. Epidemiological and clinical characteristics of 99 cases of 2019 novel coronavirus pneumonia in Wuhan, China: a descriptive study. Lancet 2020 Jan 30 [Epub ahead of print].
6. Huang C, Wang Y, Li X, et al. Clinical features of patients infected with 2019 novel coronavirus in Wuhan, China. Lancet 2020 Jan 24 [Epub ahead of print].
7. Chung M, Bernheim A, Mei X, et al. CT imaging features of 2019 Novel Coronavirus (2019-nCoV). Radiology 2020 Feb 4:200230 [Epub ahead of print].
8. Song F, Shi N, Shan F, et al. Emerging Coronavirus 2019-nCoV Pneumonia. Radiology 2020 Feb 6:200274 [Epub ahead of print].
9. Lei J, Li J, Li X, Qi X. CT Imaging of the 2019 Novel Coronavirus (2019-nCoV) Pneumonia. Radiology 2020 Jan 31:200236 [Epub ahead of print].
10. Müller NL, Ooi GC, Khong PL, Nicolaou S. Severe acute respiratory syndrome: radiographic and CT findings. AJR Am J Roentgenol 2003;181(1):3–8.
11. Wong KT, Antonio GE, Hui DS, et al. Thin-section CT of severe acute respiratory syndrome: evaluation of 73 patients exposed to or with the disease. Radiology 2003;228(2):395–400.
12. Ooi CGC, Khong PL, Ho JC, et al. Severe acute respiratory syndrome: radiographic evaluation and clinical outcome measures. Radiology 2003;229(2):500–506.
13. Munster VJ, Koopmans M, van Doremalen N, van Riel D, de Wit E. A Novel Coronavirus emerging in China - key questions for impact assessment. N Engl J Med 2020 Jan 24 [Epub ahead of print].